To be published: *IEEE Transactions on Components, Packaging and Manufacturing Technology*, 2011

The Thermal Cycling Ramifications of Lead-Free Solder on the Electronic Assembly Repair Process

Andrew Chaloupka, Peter Sandborn, and Anthony Konoza
CALCE Electronics Products and Systems Center
Department of Mechanical Engineering
University of Maryland
College Park, MD 20742 USA

Abstract - **The conversion from tin-lead to lead-free electronics has created concern amongst engineers about the reliability of electronic assemblies and the ramifications that reliability changes may have on the life cycle cost and availability of critical systems that use lead-free electronics.**

In order to analyze the impact of the tin-lead to lead-free electronics conversion in terms of life cycle cost and availability, a simulation of fielded electronic systems to and through a board-level repair facility was created. Systems manufactured with tin-lead parts or lead-free parts that are fielded, fail and have to be repaired are modeled. The model includes the effects of a finite repair process capacity, repair prioritization, multiple possible failure mechanisms, no-fault-founds, and un-repairable units. The model is used to quantify and demonstrate the system- and enterprise- level risks posed by the conversion from tin-lead to lead-free electronics.

Example analyses were performed on electronic assemblies that use SAC (tin, silver and copper) and tin-lead solder using a repair process modeled after a NSWC Crane Aviation Repair Process (8000 assemblies with 30 year support lives were modeled). The components considered consisted of Ball Grid Array (BGA), Column Grid Array (CGA) and Leadless Chip Carrier (LCC) packaged parts that experienced three different thermal cycling profiles. The case studies revealed that when exposed to usage profiles characteristic of consumer electronics, low maximum and mean thermal cycling temperatures with long dwell times, SAC exhibited significantly reduced repair costs compared to tin-lead. For usage profiles characteristic of aerospace and high-performance applications, high maximum and mean thermal cycling temperatures with short dwell times, SAC exhibited significantly increased repair costs when compared to tin-lead.

Index Terms - Lead-free electronics, Repair Simulation, RoHS, AHP, cost, availability

I. INTRODUCTION

The impact of transitioning from tin-lead to lead-free solder parts is affecting the electronics industry and most severely the aerospace and defense industries that produce products that require high levels of reliability. Products produced for applications known as AHP (Aerospace and High Performance) [1] are characterized by severe or harsh operating environments, long service times, and high consequences of failure [2]. Due to the high consequences of failure, AHP systems are currently excluded from the Restrictions on Hazardous Substances (RoHS) directive [3,4]. The current directive excludes equipment solely for the purpose of national security and military purposes that are not included in the consumer categories described in the RoHS Directive.

Although excluded from requirements to use lead-free parts, most defense and aerospace manufacturers must utilize the same supply chain as commercial electronics manufacturers for parts and boards. While the supply chains can still produce legacy products that use tin-lead solder, they have relatively little motivation to continue to

do so because the defense and aerospace industry represent less than 5% of the total market share [5]. As a result, commercial manufacturers are focused on providing lead-free parts for the commercial electronics industry. The limited availability of lead-based items has become a major driver in the design and sustainment of defense and aerospace systems as the number of tin-lead electronic suppliers has decreased. This challenge will require the defense and aerospace industry to convert to lead-free long before the RoHS directive requires it to (if ever), i.e., their current exclusion from RoHS is effectively a moot point. Irregardless of the reasons for conversion from tin-lead to lead-free electronics, the conversion is a reality and the ramifications of the conversion need to be understood.

Many AHP lead-free products will be serving in platforms where long-term (greater than 15 years) reliability is a critical requirement. For these long field life systems, the impact of reliability may be most prevalent at the system-level and enterprise-level when the sustainment (support) of products must be considered. Enterprise-level impact, refers to the impact on support logistics (sparing and repair flow: repair time, repair cost, backlog) over the support life cycle of a larger population of systems. The impact of the conversion to lead-free must be quantified in order to provide performance expectations and provide risk mitigation if and when needed to program-level management.

The next section of this paper discusses the motivation behind the development of the repair-process model described in this paper. The development is followed in Section III by a description of the model, and a detailed thermal cycling case study performed in Section IV.

II. MOTIVATION

Engineers communicate to program-level management every day that the "sky is falling" due to some previously unforeseen technical issue (lead-free, tin whiskers, counterfeit parts, obsolete parts, etc.), but management is rarely moved to action without a quantitative demonstration of the system-level and/or enterprise-level risks posed by the issue. The potential for reduced and less predictable reliability of lead-free electronics increases the probability that a serious technical issue will arise. While engineers have the resources to model and quantify system reliability, they often lack the ability to articulate the risk/impact of the reliability (or changes to the reliability) in terms of life cycle cost and availability that management will understand. In order to provide engineers with the information and knowledge to develop sound proposals (i.e., business cases) to program-level

management, a model is needed. This model needs to track populations of LRUs from field introduction to retirement (end of support) and accumulate characteristics of the failures and associated repair processes, including repair cost, repair time and availability. Where an LRU is defined as a "Line Replaceable Unit", i.e., an electronic card or board that can be removed from the field for repair or replacement. The acronym LRU is used in this paper synonymously to Shop Replaceable Assembly (SRA), Shop Replaceable Unit (SRU), and Weapon Repair Assembly (WRA). In addition to tracking a population of LRUs, it is important to provide a comparison of traditional tin-lead and lead-free solder reliability. This will allow engineers to make a direct comparison of tin-lead and lead-free solders and assess the impact on cost and availability over an entire field life for an entire population of systems.

III. Repair Process Modeling

This section describes the development of a discrete-event simulation based repair model that can be used to evaluate the repair of tin-lead and lead-free based electronic systems.

In the area of repair process modeling, a great deal of effort has been dedicated to solving classical repair problems such as "the military logistics problem of stocking repairable parts for aircrafts at bases which are capable of repairing some, but not all broken parts, and at a central depot which serves all of the bases" [6]. This method of understanding, based on Sherbrooke's METRIC model [7,8], identifies a perspective of the repair process as multi-echelon, and multi-indenture, focusing entirely on inventory constraints and replenishment quantities. Later models such as VARI-METRIC [9] are extensions to the base METRIC model that include modifications to study batch repairs and lateral shipments. These models assist in treating the logistics portion of the problem; however, they do not focus on the details of the repair process itself.

Considerable work has been done to model repair centers using discrete event simulation. An example model that was developed by Adler [10] identifies the repair center as a complex queuing situation, consisting of different service engineers (servers) of varying skills (variable service rate) that are available at different times of the day and days of the week. Similar work has been done by Ching and Zhou [11] who developed a strong queuing model that has been used to study the optimum number of operators allocated for repairing machines in order to maximize profit. While these and other models exist for repair simulation, they do not quantify the metrics of repair cost, availability and repair time that are necessary to assess the ramifications of lead-free solder.

The model described in this paper tracks information regarding individual LRUs from field introduction to end of support, to and through a repair facility. The model, described in Fig. 1, starts on the earliest date for introducing LRUs into the field. Upon fielding an LRU, the simulation samples multiple reliability distributions (representing various failure mechanisms), which are the future failure dates for the LRU. The earliest failure date causes the LRU to enter the repair process. Entering the repair process may or may not stop the "clock" associated with the other failure mechanisms that are not responsible for the failure. The length of the repair process is determined by the failure mechanism that caused the failure, part type, individual process step times, and the capacity of the repair process steps (the number of LRUs that can be accommodated concurrently may be different for each step). After the repair process is complete, the LRU returns to the field and the corresponding post-repair reliability distribution (which can differ from the original reliability distribution) is sampled for the mechanism that caused the failure and considered along with the other previously sampled failure dates (from the other failure mechanisms that did not cause the preceding failure) to determine the next failure date. If the LRU should fail again, it will undergo the repair process a second time. This process continues until the end of support date for the last LRU in the population is reached. This process, although described in terms of a single LRU, happens concurrently for the whole population of LRUs.

Each LRU is tracked independently with unique time-to-failures (TTFs) samples, repair costs, availability, and priority. The analysis is run simultaneously for all LRUs in a given time step (analyzing all LRUs at the time step before moving to the next time step) until the end of support date for the last LRU is reached. The multiple LRUs in the population are treated independently except within the repair process where only a finite number of LRUs can be

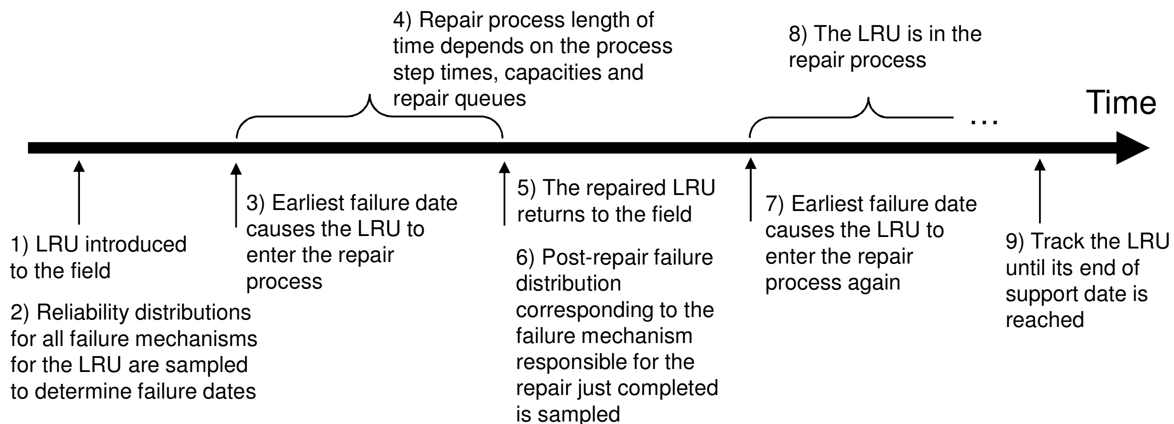

Fig. 1. Timeline of the repair simulation process for a single LRU.

concurrently addressed by each process step (resulting in queuing and sorting in step 4 as shown in Fig. 1).

A. Repair Process Modeling

A process flow is a chronological sequence of events used to describe both informational and physical objects. The repair process can be modeled as a simple process that is dictated by a sequence of process steps in a process flow. Each process step is defined by six unique properties: step name, cost, duration, capacity, failure mechanism applicability, and early retirement abilities. These properties, which are inputs to the model, affect how failed LRUs are treated by the step. Each process step is independent with respect to another process step's properties and each step has a unique position in the sequence of process steps.

Each process step's capacity dictates the maximum number of LRUs that the step can simultaneously process. If more LRUs need to concurrently use the step than the capacity allows, then the LRUs have to wait in a queue. The queue represents the sequential list of LRUs waiting to be processed by the step. LRU instances enter into the queue in the order in which they arrive at a specific process step and are addressed by the step using a FIFO (First-In, First-Out) policy unless otherwise specified by LRU repair priority. Priorities are used to sort the LRUs within a process step's queue. LRUs deemed urgent are allowed to move to the front of the queue followed by high, medium and low priority LRUs. After an LRU has completed the process step it moves on to the next step in the repair process.

The applicability of process steps may be limited based on the failure mechanism (and/or part type) that caused the LRU's failure; consequently, not every step in the repair process will be executed for every LRU.

In some cases, an LRU will enter the repair process, pass through one or more steps and be deemed non-repairable. Early retirement is supported in the model by creating specific process steps with the capability to specify a fixed fraction or distribution of LRUs to be retired. When a failed LRU enters one of these specific process steps and is determined to be retired early, the model adds a permanent spare LRU to replace the retired LRU. The failure date of the original LRU becomes the introduction date of the spare LRU. All other LRU-specific properties of the spare, including the end of service date and priority, are the same as the originally retired LRU.

Since the model's execution is based on the advancement of time, all model inputs that define events must also be mapped to time. When a non-time based reliability distribution is used, e.g., one that is in cycles (thermal, vibration or other), the model converts all values into relevant time measures based on the operational characteristics of the LRUs.

The process of determining the time step value (length) is controlled by two factors, the required accuracy of the simulation and the duration (time) of each repair process step. To obtain the best accuracy while minimizing the run-time of the simulation, the size of the time step is set to the greatest common divisor (GCD) of the process step durations during the repair process. When there are no LRUs in the repair process, the time step is set to the difference between the earliest next time to failure (TTF) and the current date.

A simplified sparing process is assumed in the model. When an LRU fails and enters the repair process, a spare is assumed to take its place in the field. However, the simulation does not accumulate time (or other environmental stresses) against the spare's failure mechanisms unless the spare becomes a permanent replacement for the LRU, i.e., only if the original LRU is retired during repair.

B. Output Metrics

In this model, the cost being calculated only represents a subset of the total ownership cost of a LRU, the cost of maintaining LRUs in the field. Other costs associated with the LRU are not addressed in this model. The repair cost per LRU is calculated by summing the cost of each repair step that the LRU was processed in. The cost of performing a repair process step is represented by the cost of performing the step during the first year (C_{repair}). A discount rate, is taken into account for repairs that occur after the first year. In (1), the present value of the cost of the repair step is calculated based on the date (D) in years after the first year of the repair and the discount rate, r.

$$C_{repair_{PV}} = \frac{C_{repair}}{(1+r)^D} \tag{1}$$

The specific process steps that each LRU undergoes are dependent on the mechanism that caused failure. LRUs may fail more than once and therefore be repaired more than once, possibly following different paths through the repair process each time they are repaired. Note: the repair of multiple failure mechanisms during one visit to the repair process is not currently supported in the model.

Availability is the probability that an item will be able to function (i.e., not failed or undergoing repair) when called upon to do so. Availability is a function of an item's reliability (how often it fails) and its maintainability (how quickly it can be restored to working order) and only applies to "repairable" systems. Quantitatively, availability is given by:

$$A = \frac{T_{up}}{T_{up} + T_{down}} \tag{2}$$

Where T_{up} is the time that the system is "up" and available for use, and T_{down} is the time that the system is not functional and not available for use when needed. Within this model, availability is defined as the fraction of time the LRU is available for field use and is calculated at the LRU level not the system level.[1] From this perspective, availability is only a function of total time in the field and the total repair time. In order to calculate the average LRU availability, each individual LRU's availability must first be determined. The individual LRU availability is calculated in (3) by subtracting the total repair time from the total time in the field and dividing this by the total time in the field.

$$A_{LRU} = \frac{\sum T_{field} - \sum T_{repair}}{\sum T_{field}} \tag{3}$$

where $\sum T_{field}$ is the total operation time in the field (30 years in the case study in Section IV) and $\sum T_{repair}$ is the sum of all the time that the LRU spends in the repair process during its lifetime. Note (3) is calculated separately for each individual LRU in the population.

IV. Case Study

The test case implemented a board with several different electronic components of various sizes and package types, and was assessed for both tin-lead and lead-free solder finishes. The objective of the test case is twofold: 1) to assess the cost and availability impact of the conversion from tin-lead to lead-free under various thermal cycling conditions, and 2) to demonstrate the capability of the model described in this paper.

The case study tracks 8000 LRU level avionics boards from introduction to retirement. Each of the 8000 LRUs were tracked independent of one another and only interact through their concurrent use of the same repair process. The test cases require three basic inputs:

1) Fielding inputs: Introduction and retirement schedules for the LRUs (how many are fielded, when they are fielded and when they are retired from the field)

2) Relevant failure mechanisms for the LRUs (represented using independent reliability distributions)

[1] Availability can be evaluated either for the LRUs or for the "sockets." Sockets are the places in a system where the fielded LRUs are located. In this model, only the availability of the LRUs is considered.

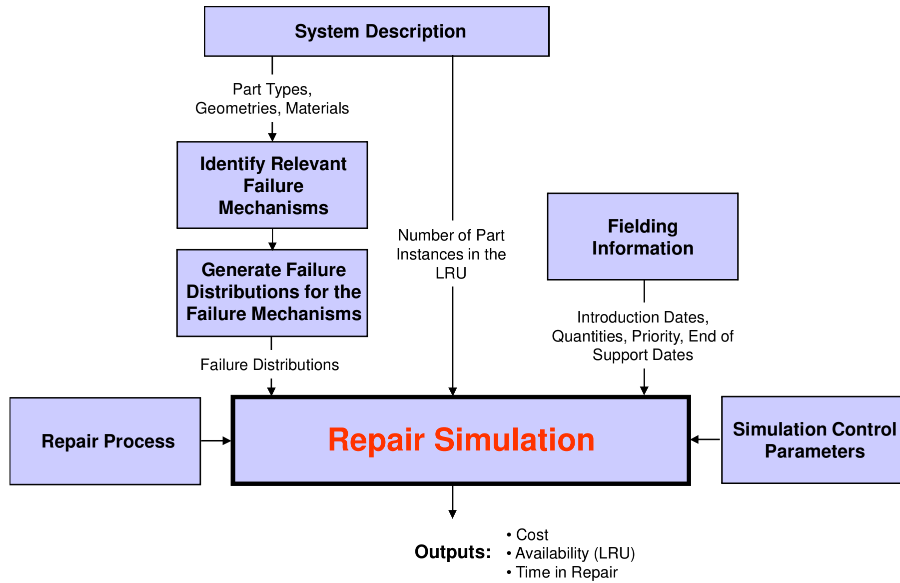

Fig. 2. Repair simulation usage model.

3) The repair process used for the LRUs (process steps including durations and capacities)

Fig. 2 shows the usage model for the repair simulation described in Section III.

A. Test Board and Packages

The packages (Table I) included for this test case consists of a ball grid array (BGA), column grid array (CGA), and a leadless chip carrier (LCC).

TABLE I
RELEVANT PACKAGE PARAMETERS

Package Parameter	BGA	CGA	LCC
Number of I/O	256 full grid (228 actual)	576 full grid	44
Interconnect Span – x (mm)	24.18	58.4	4.33
Interconnect Span – y (mm)	24.18	58.4	4.33
Package Thickness (mm)		2.4	
Package Material	Plastic	Ceramic	Ceramic
Collapsed Ball Height (mm)	0.562	-	-
Solder Height (mm)		0.1	0.1
Solder Joint Bond Area (mm^2)		0.8	
Interconnect Pitch (mm)	1.61	2.54	0.4
Interconnect Material		Alloy 42	
Column Height (mm)	-	1.7	-
Column Diameter (mm)	-	0.7	-

An LRU is capable of failing from multiple different failure mechanisms [12]. The failure mechanisms are represented in the model developed in this paper by time-to-failure (TTF) distributions. The TTF distributions

corresponding to specific failure mechanisms can be determined experimentally or from previously developed reliability models. In this paper, the applicable reliability distributions were determined using the calceFAST simulation tool [13]. The calceFAST (Failure Assessment Toolkit) is a collection of analysis models that can be used in the assessment of time to failure of structures found in electronic products and systems.

In order to develop a test board with failure characteristics similar to experimental boards containing similar components, calceFAST was calibrated. The Monte Carlo TTF data generated from calceFAST[2] was fit to a Weibull distribution using Weibull++ [14], using the following process assuming first order thermal fatigue failure models.[3] An experimental case comprised of a 228 lead BGA package that experienced 0 to 100 °C thermal cycling with 10-minute dwell times was used to calibrate the Weibull distribution values from calceFAST. Two parameters, the thermal calibration factor and interconnect length were adjusted in calceFAST to calibrate the simulated distributions to the experimental results from [18], see Fig. 3. In calceFAST, all instances of the test packages were

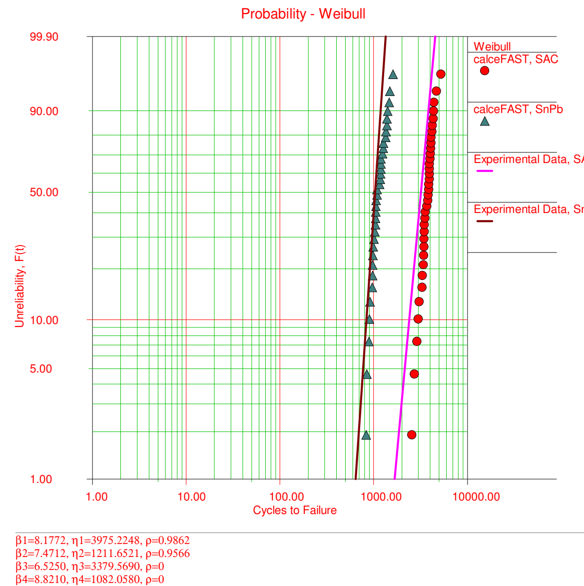

Fig. 3. Calibrated calceFAST simulations and experimental TTF data, from [18] for a 228 lead BGA package.

[2] The height of the solder connection was varied in calceFAST in the Monte Carlo analysis in order to emulate variations in the solder material and other manufacturing variations.

[3] The models assume failure occurs at the solder joint between the package and printed wiring board. In the case of the CGA and LCC packages, the models calculate the median cycles to failure in the solder joint modeled as a simple pillar subjected only to in-plane deformation using calculated average shear strain. Failure is assumed to obey a power law relation and the fatigue exponent was evaluated by Engelmaier [15] for near eutectic tin lead solders using Wild's solder data [16] and for tin-lead solders using data in [17]. In the case of the BGA, a full array is assumed and the model examines the failure of the die shadow solder ball, as well as the outer perimeter solder ball. The lower value of the two inspection points is reported. In all cases, the models contain a thermal calibration factor (scalar of the strain) that can be adjusted (a value of 1.5 was used for all the cases in this paper). For BGA and LCC package types, the first order thermal fatigue model does not depend on the package thickness or solder joint bond area, so they are not included in Table I.

cycled until failure. The sample size for the Monte Carlo simulation was based on convergence of the Weibull parameters. The LCC and CGA package types were similarly calibrated to experimental results.

A study composed of three different thermal cycling profiles was performed as described in Table II. The goal of the different profiles was to evaluate a range of thermal cycling parameters where: 1) SnPb is more reliable, 2) SAC and SnPb are expected to have similar reliability, and 3) SAC is more reliable [19,20]. Parameters adjusted within the profiles included the dwell time, maximum, minimum and mean temperatures. The maximum and minimum temperatures represent the upper and lower limits of the thermal cycle. The mean is half way between the maximum and minimum temperatures. Dwell time is the length of time that a temperature is maintained at the maximum and minimum of the temperature cycle.

TABLE II
THERMAL CYCLING CASES 1-3 USED IN THE CASE STUDY

	Max Temp (˚C)	Min Temp (˚C)	Avg Temp (˚C)	Low Temp Dwell Time (min)	High Temp Dwell Time (min)
Case 1	130.0	0.0	65.0	0.1	0.1
Case 2	110.0	0.0	55.0	10.0	10.0
Case 3	100.0	0.0	50.0	40.0	40.0

Case 1 in Table II exhibits a high maximum temperature of 130 °C, a higher mean temperature of 65 °C, and a short dwell time of 0.1 minutes (6 seconds). Case 2 in Table II exhibits a medium maximum temperature of 110 °C, a medium mean temperature of 55 °C, and a medium dwell time of 10 minutes. Case 3 in Table II exhibits a low maximum temperature of 100 °C, a mean temperature of 50 °C, with a long dwell time of 40 minutes. For these three cases calceFAST predicts that: SnPb is more reliable than SAC in Case 1, SAC and SnPb have nearly identical reliabilities in Case 2, and SAC is more reliable than SnPb in Case 3. Table III summarizes the reliability distributions obtained for the packages from the calceFAST model calibrated for the three thermal cycling cases.

TABLE III
WEIBULL PARAMETERS FROM SIMULATION, β = SHAPE, η = SCALE (CYCLES), ρ = CORRELATION COEFFICIENT

BGA	Solder Type	SnPb			SAC 305		
	Weibull Parameter	β	η	ρ	β	η	ρ
	Case 1	14.3930	1349.5196	0.9543	13.2601	710.5656	0.9555
	Case 2	16.0867	733.1301	0.9550	13.5834	777.9479	0.9514
	Case 3	16.4404	710.1023	0.9567	13.3239	949.4979	0.9550
CGA	Weibull Parameter	β	η	ρ	β	η	ρ
	Case 1	15.2061	1312.1411	0.9319	15.1000	560.3206	0.9370
	Case 2	17.6609	736.9550	0,9298	15.2383	645.8529	0.9337
	Case 3	18.3160	724.4178	0.9417	15.2505	808.0187	0.9341
LCC	Weibull Parameter	β	η	ρ	β	η	ρ
	Case 1	14.2055	852.7378	0.9583	12.8109	433.1598	0.9535
	Case 2	15.5269	488.8268	0.9541	14.0313	479.4791	0.9582
	Case 3	17.3595	477.0349	0.9585	13.8519	586.9142	0.9549

B. Operational and Repair Inputs

For the test cases, the LRU deployment schedule depicted in Fig. 4 was assumed. The schedule introduces LRUs quarterly over a ten-year period with a smooth introduction rate and an equivalent retirement rate during a ten year period.

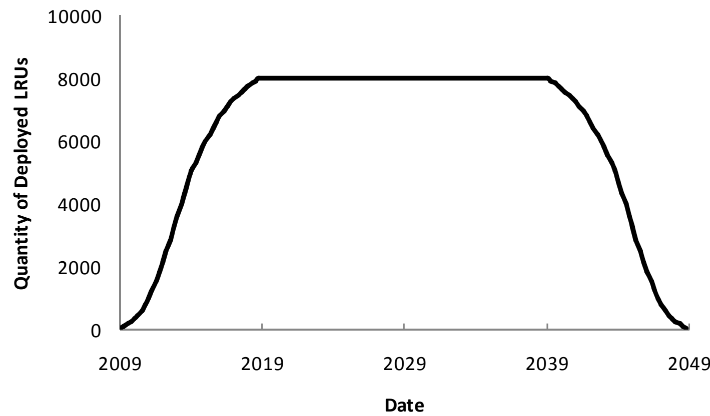

Fig. 4. Assumed deployment schedule (every LRU is in the field for exactly 30 years).

GEIA assumes that in most cases 1000 operational cycles are sufficient for estimating usage over support life and is considered a standard duration for reliability testing for aerospace systems [1]. In the test cases discussed in this paper, each LRU has a support life of exactly 30 years over which it will experience 1000 operational cycles. This equates to an operational profile of approximately 33 cycles per year.

The repair process used in this model, Table IV, was formulated based on the NSWC Crane aviation repair process [21]. The repair process contains 48 independent process steps. Specific to this repair process is a 10% probability that the LRU is NFF.[4] If a LRU is determined to be NFF, it skips steps 11 through 39 in the repair process. The assumption made in this paper is that NFFs will, on average, spend less time in the repair process than repaired failures; however, depending on the type of system this may not always be true. Steps 0 through 5 and steps 40 through 47 are considered administrative steps, such as packaging, transit and paperwork - these steps are executed regardless of the failure mechanism that caused the LRU to fail.

[4] NFF means No Fault Found. NFFs are LRUs that failed in the field, entered the repair process, and no problems with the LRU can be found in the repair process.

TABLE IV
REPAIR PROCESS

Index #	Process Step	Duration	Cost	Capacity
0	YY Field Failure ID	1.00	75.00	200
1	Capture of Resources	2.00	75.00	200
2	Removal	1.00	75.00	200
3	Package For Transit	2.00	150.00	100
4	Transit	60.00	1200.00	100000
5	Receiving	18.00	30.00	100000
6	Disassembly to Card Level	2.00	150.00	4
7	Locate Test Program	1.00	75.00	4
8	Test Prep	1.00	75.00	4
9	Run Test	0.50	37.50	4
10	Diagnose to Component	0.50	37.50	4
11	Coating Removal	0.20	100.00	4
12	Remove Part	0.30	22.50	4
13	Clean/Prep the Site	0.50	100.00	4
14	Find Parts	0.50	37.50	4
15	Pull Parts From Supply	0.10	15.00	4
16	Prep Site	0.20	50.00	4
17	Component Prep	0.20	15.00	4
18	Assemble To Card	0.30	22.50	4
19	Continuity Testing	0.20	15.00	4
20	Coating Replacement	24.00	150.00	10
21	Verify Fault Corre.	0.50	37.50	4
22	Coating Removal	0.50	500.00	4
23	Remove Part	0.70	50.00	4
24	Clean/Prep the Site	0.70	150.00	4
25	Pull Parts From Supply	0.10	200.00	4
26	Prep Site	0.40	100.00	4
27	Component Prep	1.00	200.00	4
28	Assemble To Card	1.00	75.00	4
29	Continuity Testing	1.00	75.00	4
30	Verify Fault Corre.	1.00	75.00	4
31	Coating Removal	0.30	200.00	4
32	Remove Part	0.50	37.50	4
33	Clean/Prep the Site	0.60	120.00	4
34	Pull Parts From Supply	0.10	50.00	4
35	Prep Site	0.30	75.00	4
36	Component Prep	0.50	75.00	4
37	Assemble To Card	0.50	37.50	4
38	Continuity Testing	0.40	40.00	4
39	Verify Fault Corre.	0.70	40.00	4
40	Put Box Together	2.00	150.00	4
41	Complete Paperwork	1.00	75.00	4
42	Maint. Officer Sort	1.00	75.00	1
43	Package For Transit	2.00	150.00	4
44	Transit	60.00	1200.00	100000
45	Receiving	18.00	30.00	100000
46	Reinstall	1.00	75.00	200
47	Verify Fix In System	1.00	75.00	200

Within the repair process as seen in Table IV, there are columns that specify information regarding each individual step and its relationship to the process. This is important as LRUs move sequentially from the first to the last step. The "Process Step" column defines the name of the step. The "Duration" column is the minimum time (calendar hours) required for an LRU to complete the step. The "Cost" column represents the cost ($) to perform the step on a single LRU. The "Capacity" column represents the maximum number of LRUs that can be simultaneously processed in the step. In addition, each process step can be characterized by its applicability to specific failure mechanisms and/or specific part types. For the case study presented here, every step was assumed to be applicable to every part type and failure mechanism (with the exception of the NFFs already discussed).

When determining the time spent in the repair process for each LRU, there is the implicit assumption that the repair process runs continuously when needed.

C. Analysis Results

In order to study the impact of the conversion to lead-free, the model was run independently for: 1) package types attached with SnPb solder and 2) package types attached with SAC 305 solder.

Histograms were generated for distributions of repair cost, availability, and repair time. The frequency in the histograms represents the quantity within the 8000 LRU population that shares a particular range of values.

Thermal Cycling Case 1 – High Temperature, Short Dwell Time

The case 1 data was plotted as frequency versus the metric of interest: repair cost ($) seen in Fig. 5, availability (fraction of uptime over total time) seen in Fig. 6, and repair time (days) seen in Fig. 7.

The two large populations of LRUs in Fig. 5 are a result of a varying number of failures per LRU in their 30 year field life. The majority of the LRUs in the SnPb distribution have failed only once. The majority of the LRUs in the SAC distribution have failed 3 or 4 times, which explains why their repair cost is nearly four times the SnPb

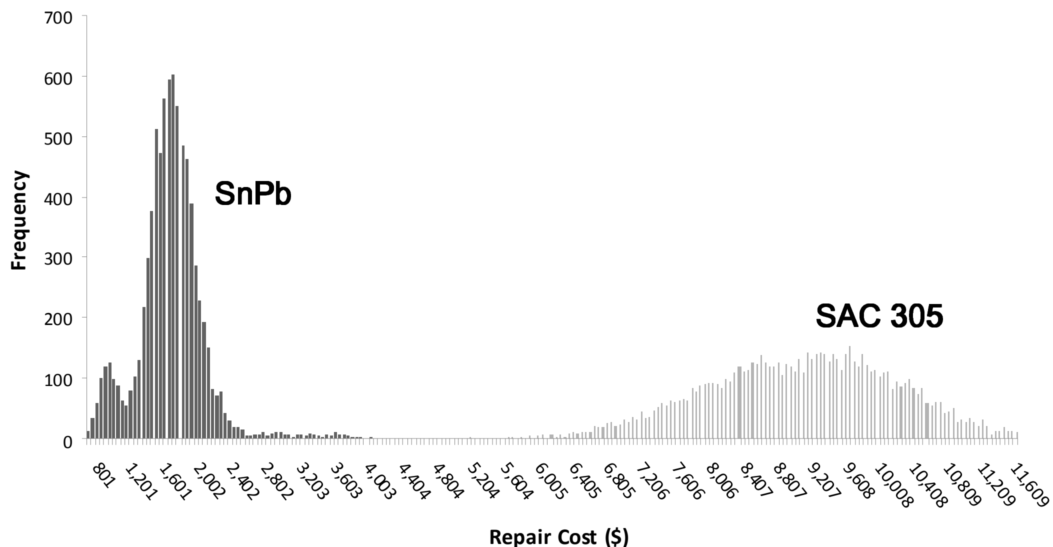

Fig. 5. Histogram comparing repair cost (per LRU) for SnPb and SAC, case 1.

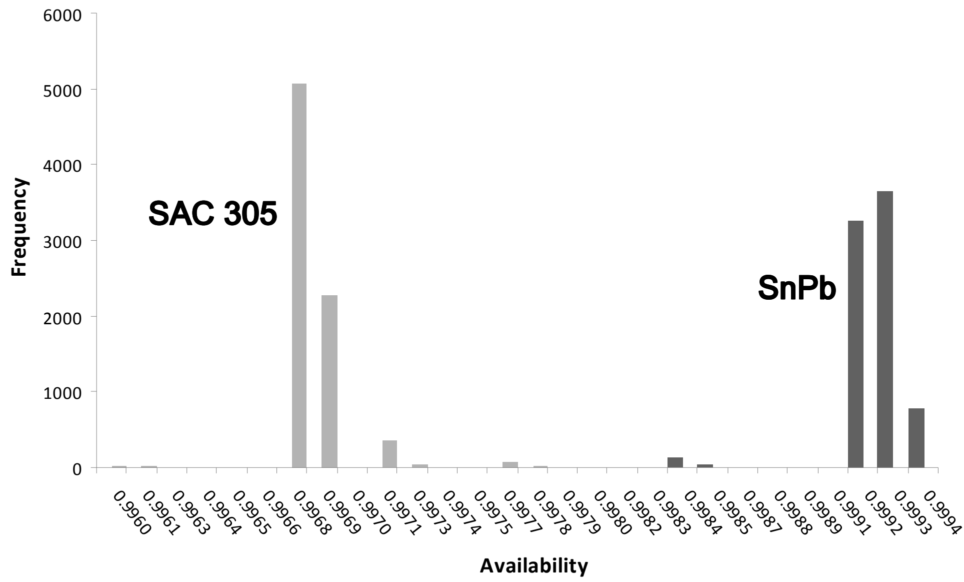

Fig. 6. Histogram comparing LRU availability for SnPb and SAC, case 1.

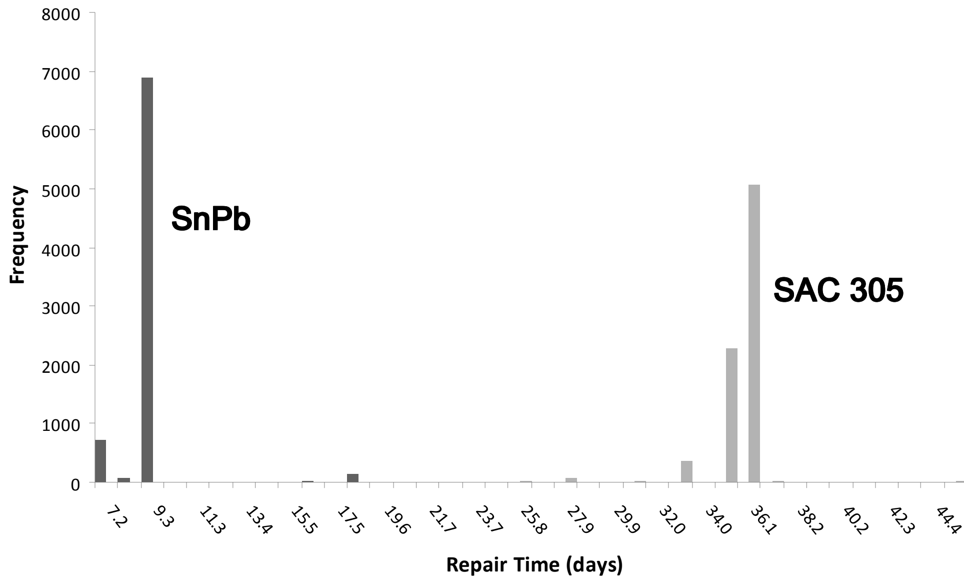

Fig. 7. Histogram comparing repair time (per LRU) for SnPb and SAC, case 1.

LRU's repair costs. Because the SnPb LRUs generally failed less than the SAC LRUs under the case 1 temperature cycling conditions, their availability is higher (Fig. 6) and the accumulated repair time is smaller (Fig. 7).

The small population between $801 and $1201 in Fig. 5 is a result of LRUs that had one or more NFFs. These LRUs are not processed in NSWC Crane repair process steps 11-39, Table IV. Therefore, their corresponding repair cost is lower than repaired LRUs that had failures.

The average repair cost per LRU for case 1 (SnPb/SAC) is $1742/$9114, average availability is 0.9991/0.9968, and the average repair time is 9.6/35.6 days. The following conclusions can be drawn from case 1 in which LRUs experienced the higher temperature, short dwell time thermal cycling: conversion from SnPb to SAC resulted in a 290.17% increase in the number of failures, a 423.14% increase in cost, 0.23% decrease in availability and a 272.29% increase in repair time by using SAC solder.

The individual LRU metrics plotted over time may also be of interest. Figure 8 shows the maximum individual LRU repair cost in the population, the minimum individual LRU repair cost in the population, and the average LRU repair cost of the population.

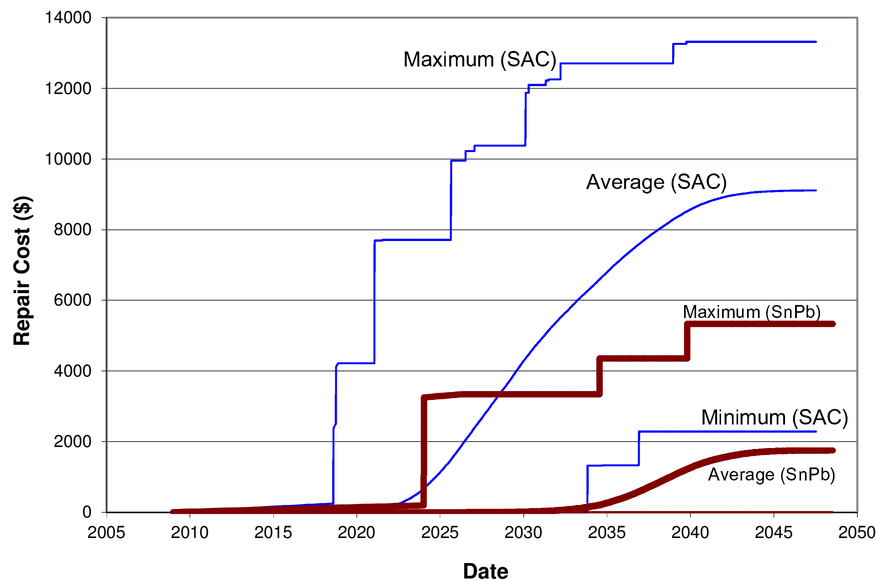

Fig. 8. Individual minimum and maximum LRU repair cost compared to the average LRU repair cost for SnPb and SAC solder. Note: there is no Minimum (SnPb) shown because it is zero.

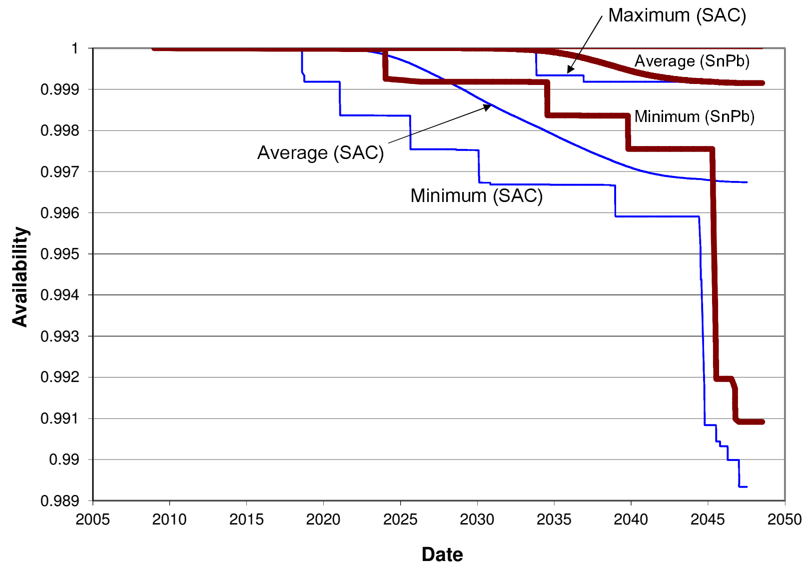

Fig. 9. Individual minimum and maximum LRU availability compared to the average LRU availability for SnPb and SAC solder. Note: there is no Maximum (SnPb) shown because it is one.

Figure 9 plots the maximum individual LRU availability, the minimum individual LRU availability, and the average LRU availability. The LRU with the minimum availability is also the LRU that has the maximum repair time and costs.

Figure 10 plots the maximum individual LRU repair time, the minimum individual LRU repair time, and the average LRU repair time. The LRU with the maximum repair time is also the LRU that has the maximum repair costs.

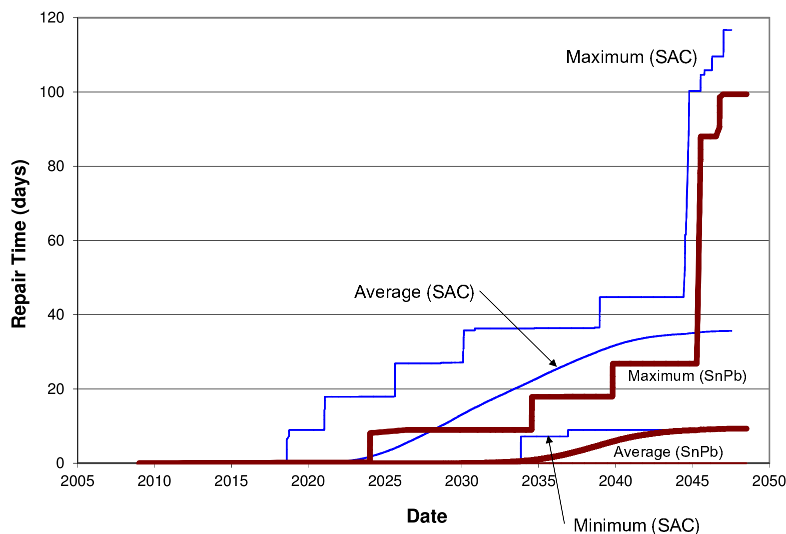

Fig. 10. Individual minimum and maximum LRU repair time compared to the average LRU repair time for SnPb and SAC solder. Note: there is no Minimum (SnPb) shown because it is zero.

Thermal Cycling Case 2 – Medium Temperature, Medium Dwell Time

The case 2 data was plotted as frequency versus the metric of interest: repair cost ($) as seen in Fig. 11, availability (fraction of uptime over total time) as seen in Fig. 12, or repair time (days) as seen in Fig. 13.

The average repair cost per LRU for case 2 (SnPb/SAC) is $7821/$8163, average availability is 0.9969/0.9969, and the average repair time is 33.9/34.5 days. The following conclusions can be made from case 2 in which LRUs experienced the medium temperature, medium dwell time thermal cycling profile: conversion from SnPb to SAC resulted in a 1.87% increase in the number of failures, a 4.38% increase in cost, no change in availability, and a 1.33% increase in repair time.

Thermal Cycling Case 3 – Low Temperature, Long Dwell Time

The case 3 data was plotted as frequency versus the metric of interest: repair cost ($) as seen in Fig. 14, availability (fraction of uptime over total time) as seen in Fig. 15, or repair time (days) as seen in Fig. 16.

The average repair cost per LRU for case 3 (SnPb/SAC) is $8175/$5523, average availability is 0.9968/0.9977, and the average repair time is 34.7/25.5 days. The following conclusions can be made from case 3 in which LRUs experienced a low temperature and long dwell time thermal cycling profile: conversion from SnPb to SAC results in

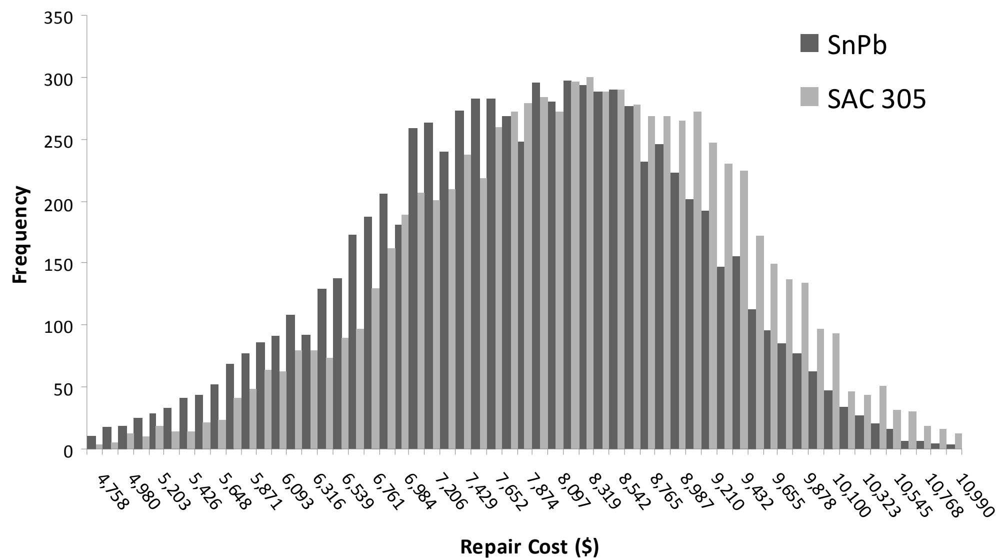

Fig. 11. Histogram comparing repair cost (per LRU) for SnPb and SAC, case 2.

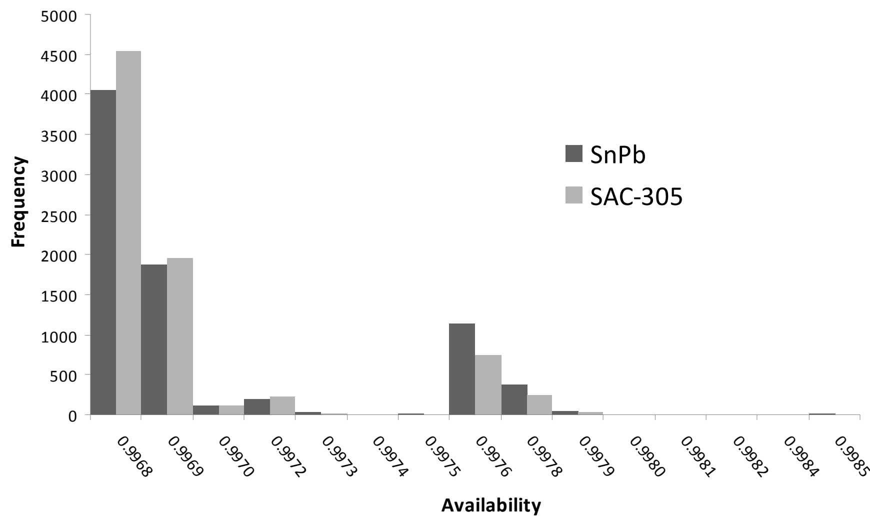

Fig. 12. Histogram comparing LRU availability for SnPb and SAC, case 2.

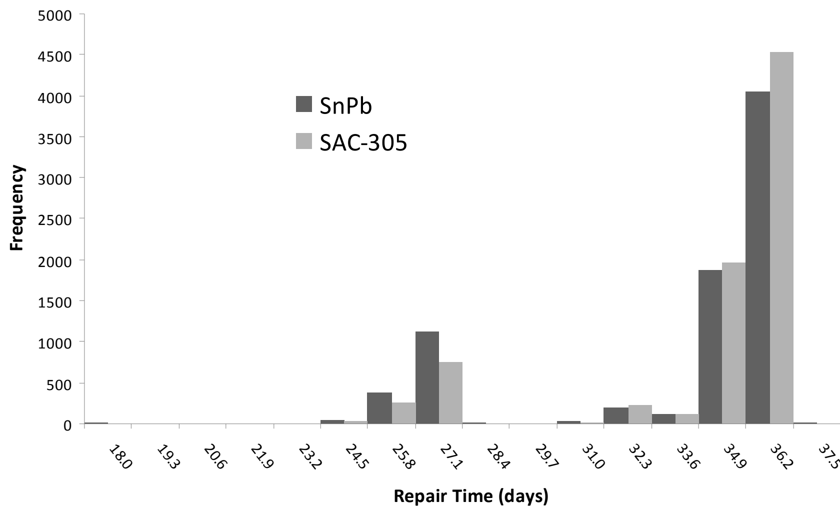

Fig. 13. Histogram comparing repair time (per LRU) for SnPb and SAC, case 2.

a 27.71% decrease in the number of failures, a 32.45% decrease in cost, a 0.08% increase in availability, and a 26.68% decrease in repair time.

The histograms in Figs. 14-16 represent a single 8000 LRU population. In order to assess the variability in the results for the population, the standard deviation of each of the average metrics was calculated over 10 separate 8000 LRU population analyses. The result is that for SnPb solder, the average number of failures differed by ±0.0036 failures per LRU, the average repair cost differed by ±\$6.40, the average availability changes insignificantly, and the average time in repair differed by ±0.10 days. For SAC solder, the average number of failures differed by ±0.0043

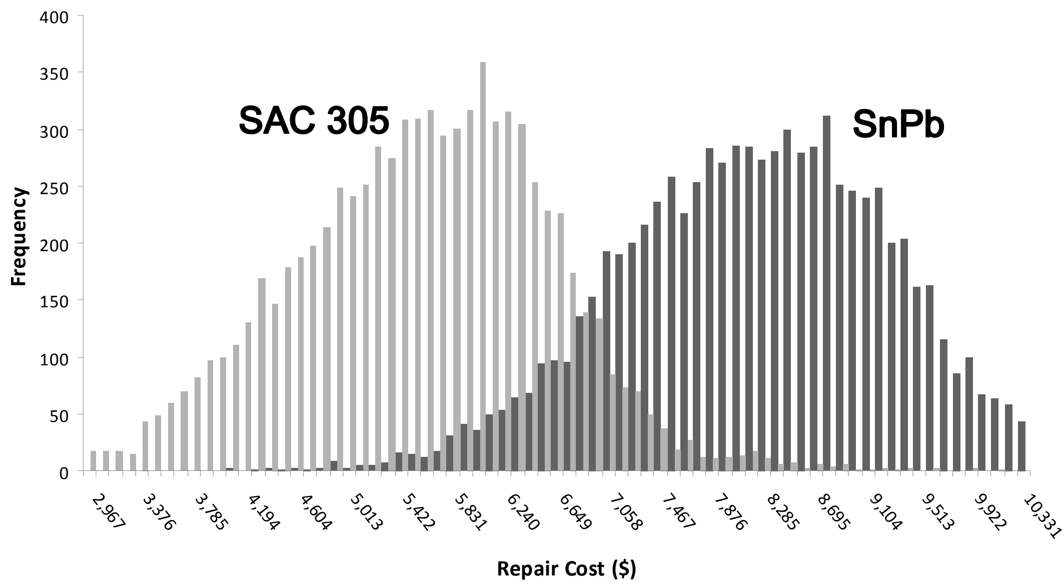

Fig. 14. Histogram comparing repair cost (per LRU) for SnPb and SAC, case 3.

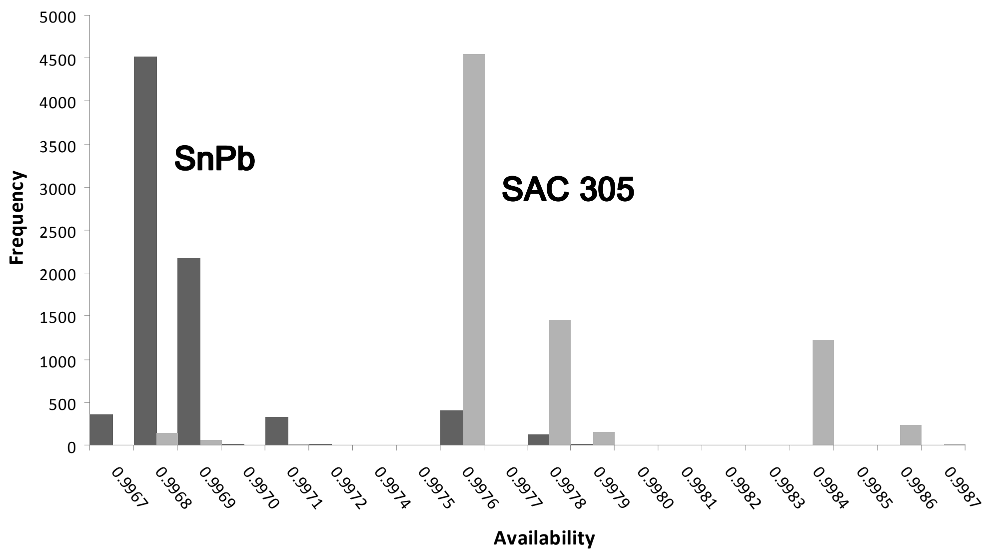

Fig. 15. Histogram comparing LRU availability for SnPb and SAC, case 3.

failures per LRU, the average repair cost differed by ±$8.81, the average availability changes insignificantly, and the average time in repair differed by ±0.17 days.

Thermal Cycling Case 1 – High Temperature, Short Dwell Time, Not Good-As-New Repair

In the first three cases considered, the repair assumption was good-as-new, meaning that the LRUs coming out of the repair process had exactly the same reliability (with respect to the failure mechanism that precipitated the

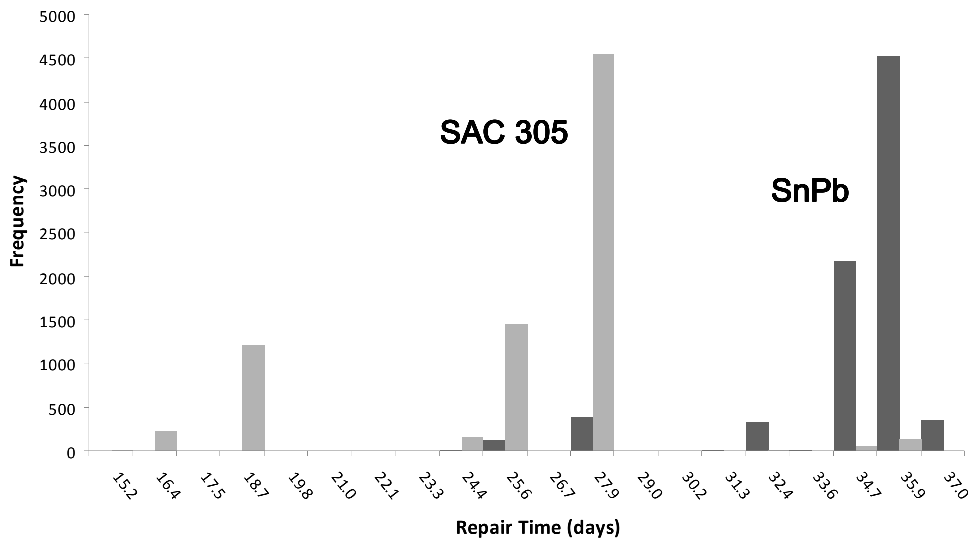

Fig. 16. Histogram comparing repair time (per LRU) for SnPb and SAC, case 3.

repair) as the original LRUs. Note: the repair process was assumed to have no effect on the damage accumulated relative to other failure mechanisms that did not precipitate the failure, i.e., their "clocks" are unaffected. In this case we assume that the repairs are not good-as-new and result in a 20% reduction in reliability (modeled as a 20% decrease in the Weibull scale parameter); experimental results in [22] suggest that the reliability of reworked plastic lead-free BGAs was 18% lower than non-reworked assemblies subjected to -55 to 125 ˚C thermal cycling conditions.

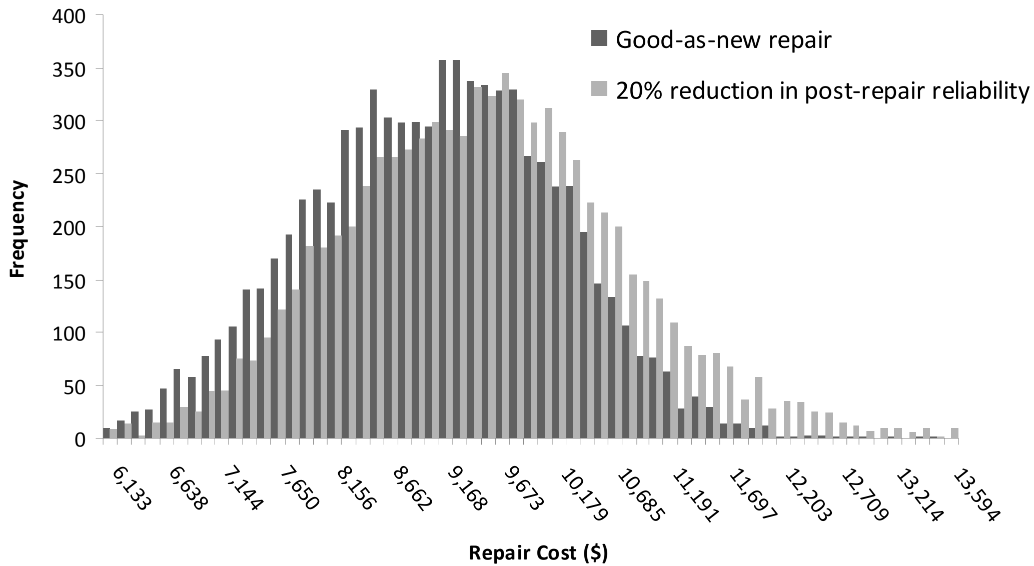

Fig. 17. Histogram comparing repair cost (per LRU) for baseline and 20% reduced post-repair reliability under case 1 thermal cycling conditions.

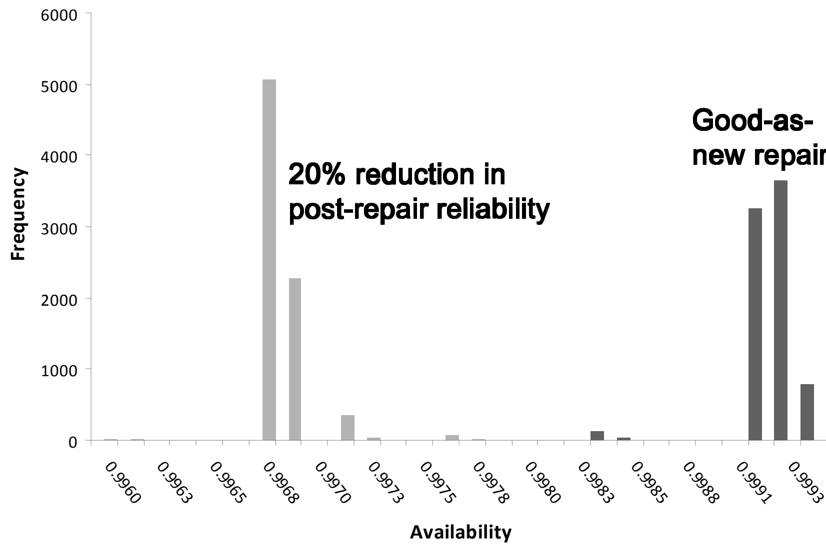

Fig. 18. Histogram comparing LRU availability for baseline and 20% reduced post-repair reliability under case 1 thermal cycling conditions.

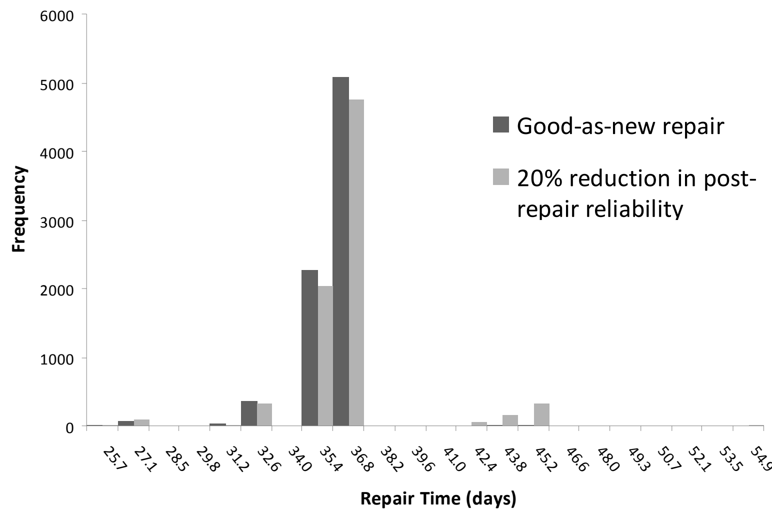

Fig. 19. Histogram comparing repair time (per LRU) for baseline and 20% reduced post-repair reliability under case 1 thermal cycling conditions.

The not good-as-new repair case data was plotted as frequency versus the metric of interest for SAC under case 1 thermal cycling conditions: repair cost ($) as seen in Fig. 17, availability (fraction of uptime over total time) as seen in Fig. 18, and repair time (days) as seen in Fig. 19.

The average repair cost per LRU for this case (good-as-new/not good-as-new) is $9114/$9436, average availability is 0.9968/0.9967, and the average repair time is 35.6/36.5 days. The following conclusions can be made from this case in which LRUs experienced high temperature and short dwell times with not good-as-new repair:

there was a 2.12% increase in the number of failures, a 3.54% increase in cost, a 0.01% decrease in availability, and a 2.76% increase in repair time by reducing the post repair reliabilities by 20%.

V. Discussion and Conclusions

The test cases considered quantify the impact of varying solder type and post-repair reliability on the repair cost, availability and repair time. Table V, summarizes the impact of each of these variables in terms of the percent difference from the baseline. For example, in cases 1-3, the difference represented is between SnPb and SAC, so 290.17% represents a 290.17% increase when changing from SnPb to SAC. In the right most case 1 column, the difference represented is between SAC with good-as-new repair and with a 20% reduction in post-repair reliability.

TABLE V
CASE STUDY RESULTS, PERCENT DIFFERENCES

Thermal Cycling Case	Case 1	Case 2	Case 3	Case 1
Special cases	SnPb relative to SAC	SnPb relative to SAC	SnPb relative to SAC	SAC only. Good-as-new repair relative to not good-as-new repair (20% post repair reliability reduction)
Avg. Number of Failures per LRU	290.17%	1.87%	-27.71%	2.12%
Avg. Repair Cost	423.14%	4.38%	-32.45%	3.54%
Avg. LRU Availability	0.23%	0.00%	0.08%	-0.01%
Avg. Repair Time	272.29%	1.33%	-26.68%	2.76%

Several system management situations are possible that are not accommodated in the model presented in this paper. Currently, the model defines the duration of each process step as a fixed value, i.e., except for delays due to queuing, the duration stays constant for all LRUs that enter a step. Actual repair process step durations are time-variant. Process step durations are also impacted by the reduced availability of replacement parts or other resources (e.g., when a part becomes obsolete, or when a lifetime buy runs out). In order to model time-variant step durations the process step durations could be represented as distributions allowing for the variability in the process and uncertainty of part availability.

A special situation exists in the simulation when two or more reliability distributions for a LRU share the same sampled TTF date. Currently, the simulation processes multiple failure dates that share the same date as a single LRU failure. Multiple simultaneous failures in the same LRU should be addressed differently than a single failure, or multiple non-simultaneous failures since particular steps in the repair process are common to the LRU and not

specific to the part type that failed. Many of the process steps, such as packaging and shipping, can be combined to reduce the cost of multiple repairs.

The repair simulation described in this paper has potential applications beyond quantifying the ramifications of the conversion from tin-lead to lead-free solder. For example, the simulator developed in this model could be used as the basis for a tradeoff model for electronic systems that allows an assessment of the practicality of treating a LRU as a 'throwaway' or disposable item.

ACKNOWLEDGMENT

This work was supported in part by the CALCE Electronic Products and Systems Consortium. The authors also wish to thank Bill Russell at Raytheon and Denny Fritz at SAIC for their contributions to this research, and the Naval Surface Warfare Center at Crane Indiana for providing data and technical feedback.

REFERENCES

[1] GEIA-STD-0005-3 Draft 50, "Performance testing for aerospace and high performance electronic interconnects containing Pb-free solder and finishes," April 29, 2008.
[2] GEIA-HB-0005-2, "Technical Guidelines for Aerospace and High Performance Electronic Systems Containing Lead-Free Solder and Finishes," November 1, 2007.
[3] European Union, (2002/95/EC), "Directive 2002/96/EC of the European Parliament and of the Council of 27 January 2003 on Waste of Electrical and Electronic Equipment," *Official Journal of the European Union*, pp. L37/24-L37/38.
[4] European Union, (2002/96/EC), "Directive 2002/95/EC of the European Parliament and of the Council of 27 January 2003 on the Restriction of the Use of Certain Hazardous Substances in Electrical and Electronic Equipment," *Official Journal of the European Union*, pp. L37/19-L37/23.
[5] B. Russell, D. Fritz, and G. Latta, "Methodology for evaluating data for 'reverse compatibility' of solder joints," in *Proc. SMTA International*, October 2007.
[6] D. Guide and R. Srivastava, "Repairable inventory theory: Models and applications," *European Journal of Operational Research*, vol. 102, pp. 1-20, 1997.
[7] C. Sherbrooke, "METRIC: A multi-echelon technique for recoverable item control," *Operations Research,* vol. 16, no. 1, pp. 122-141, 1968.
[8] W. Kennedy, J. Patterson, and L. Fredendall, "An overview of recent literature on spare parts inventories," *International Journal of Production Economics*, vol. 76, pp. 201-215, 2002.
[9] M. Slay, "VARI-METRIC: An approach to modeling mult-echelon resupply when the demand process is Poisson with a Gamma prior," *Working Paper, Logistics Management Institute*, Washington DC, July 1980.
[10] G.L. Adler, "The use of a repair center simulation," in *Proc. of the 5th Winter Simulation Conference*, 1971, pp. 131-137.
[11] W.K. Ching and X.Y. Zhou, "Machine repairing models for manufacturing systems," in *Proc. of the 5th IEEE Conf. on Emerging Technologies and Factory Automation*, 1996, pp. 221-226.
[12] A. Dasgupta and M. Pecht, "Material failure mechanism and damage models," *IEEE Transactions on Reliability*, vol. 40, no. 5, pp. 531-536, 1991.
[13] *CalceFAST* Vers. 5.0. College Park, MD: CALCE EPSC, 2005.
[14] Weibull++, Vers. 6. Reliasoft, 2003.

[15] W. Engelmaier, "Chapter 17: Solder attachment reliability, accelerated testing, and result evaluation," *Solder Joint Reliability - Theory and Applications*, edited by J. H. Lau, Van Nostrand Reinhold, New York, NY, Nostrand Reinhold, New York, pp. 545-587, 1991.
[16] R.N. Wild, "Some fatigue properties of solders and solder joints," *IBM Technical Report 73Z000421*, January 1973.
[17] S. Yoon, Z. Chen, M. Osterman, B. Han, and A. Dasgupta, "Effect of stress relaxation on board level reliability of Sn based Pb-free solders," in *Proc. of the Electronic Component and Technology Conference,* Orlando, FL, June 2005, pp. 1210-1214.
[18] DfR Solutions, "2nd generation LF alloys Is SAC the best we can do?" June 22, 2009. From: http://www.dfrsolutions.com/uploads/publications/2009_06_2nd%20Generation%20LF%20Alloys-PPT.pdf
[19] L. Everhart, P. McCluskey, P. Hansen, C. Vrignaud, P. Lewandowski, and S. Ramminger "PoF reliability assessment of an engine control unit," in *Proc. of 2nd Int'l SIA Conf. on Automotive Power Electronics*, Paris, France, Sept. 2007.
[20] P. McCluskey, P. Hansen, C. Lenakakis, and W. Wondrak, "Virtual qualification using field life temperature data," in *Proc. of ASME InterPACK*, San Francisco, CA, July 2009.
[21] Naval Air Systems Command, *Standard Maintenance Practices Miniature/Microminiature (2M) Electronic Assembly Repair*, 2006.
[22] L. Nie, M. Osterman, and M. Pecht, "Microstructural analysis of reworked ball grid array assemblies under thermomechanical loading conditions," *IEEE Trans. on Devices and Materials Reliability*, vol. 10, no. 2, pp. 276-286, June 2010.